RSC Advances

ROYAL SOCIETY OF CHEMISTRY

www.rsc.org/advances

Table of contents entry

Electrospun Acid-Base Pair Solid Dispersions of Quercetin

Jie Yan, Yong-Hui Wu, Deng-Guang Yu, Gareth R. Williams, Shang-Meng Huang, Wen Tao, and Jun-Yi Sun

An electrospun acid-base pair solid dispersion in the form of core-shell nanofibers was developed for improving the dissolution of quercetin

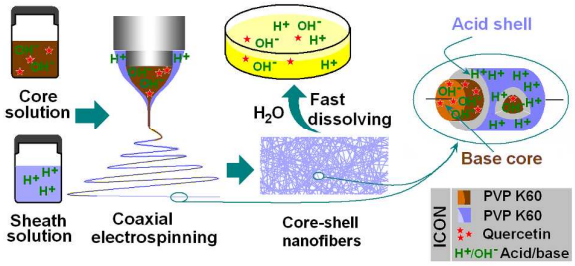

(8 cm× 4 cm, 600 dpi)

Cite this: DOI:

www.rsc.org/xxxxxx

ARTICLE TYPE

Electrospun Acid-Base Pair Solid Dispersions of Quercetin

Jie Yan *[a], Yong-Hui Wu,[b] Deng-Guang Yu,*[c] Gareth R. Williams,*[d] Shang-Meng Huang,[b] Wen Tao,[c] and Jun-Yi Sun[c]

Received (in XXX, XXX) Xth XXXXXXXXX 201X, Accepted Xth XXXXXXXXX 201X

DOI: 10.1039/b000000x

In this work, electrospinning was used to fabricate core-shell nanofibers containing acid-base pairs. Quercetin was used as a model active ingredient. To exploit its solubility in basic conditions, a solution of quercetin, polyvinylpyrrolidone (PVP) and sodium hydroxide was used as the core fluid, and one consisting of citric acid and PVP as the shell fluid. Scanning and transmission electron microscopy demonstrated that core-shell nanofibers with linear morphologies were obtained, without beads or spindles. X-ray diffraction showed that quercetin was present in the fibers in an amorphous state; Fourier transform infrared spectroscopy indicated this may be a result of hydrogen bonding between the drug and the polymer matrix. In *in vitro* dissolution tests the drug was found to be released immediately when the fibers encountered an aqeuous medium. There was no change in the pH of the medium after dissolution, as a result of the presence of the acid-base pair. This provides a new strategy for improving the dissolution behavior of poorly water-soluble drugs using polymeric nanostructures.

1. Introduction

Electrospinning is a facile technique which has been widely explored for the generation of polymer nanofibers and polymer-based nanocomposites over the past decade.[1-5] The working fluid in a traditional single fluid electrospinning process is often a mixed solution of an active ingredient and a filament-forming polymer; suspensions of functional nanoparticles may also be used.[6-10] The active ingredient must have sufficient solubility in the chosen solvent to give an effective therapeutic dose in the patient. The polymer should have good filament-forming properties and be soluble at an adequate concentration to permit the formation of fibers. This greatly limits the development of functional materials based on monolithic electrospun fibers, because only a limited number of polymer/solvent combinations yield fibers. Fortunately, coaxial electrospinning, in which two fluids can be co-electrospun simultaneously, can overcome this limitation because only one fluid need to be electrospinnable for the process to proceed successfully and generate nanofibers.[11-13] Moreover, co-axial spinning provides fibers with "core/shell" structures and the possibility of spatially tailoring the locations of the components within the fibers .[14-16]

Single fluid electrospinning processes have been widely reported for the development of novel solid dispersions (SDs) of poorly water soluble drugs, aiming to improve their dissolution properties.[17-19] These nanofiber-based SDs include double-component SDs consisting of an active ingredient and a polymer matrix and multiple-component SDs containing a drug, a polymer, a surfactant, and a sweeter. [17,20] The SDs produced could release the incorporated active ingredients immediately when they encountered water. However, it is impossible to develop this type of SD for some drugs owing to their very low solubility in the typical organic solvents that are suitable for preparing electrospinnable polymer solutions. Most recently, a coaxial electrospinning process has been demonstrated to provide a solution to this problem, through which a new type of SD in the form of core-shell nanofibers was prepared. In this process, an unspinnable core fluid consisting of acyclovir and polyvinylpyrrolidone (PVP) in a solution containing N,N-dimethylacetamide (DMAc) could be converted into fibers if the sheath fluid was spinnable. [21]

Poorly water-soluble drugs are used in over 40% of currently available medical products; 60% of active ingredients under development are also poorly water soluble. [20,22] Many of these drugs are ionisable, and hence their solubility can be enhanced by varying the pH, or by salt formation. Examples include N-acetyl-p-aminophenol, acyclovir, tamoxifen, itraconazole and amiodarone.

Here we report a new type of electrospun acid-base pair SDs (AB-SDs) for poorly water-soluble active ingredients, which were fabricated using a coaxial electrospinning process. Quercetin was used as a model poorly soluble drug. It is a flavonoid found in many foods and plants and which has been explored for treating a range of different diseases such as high cholesterol, heart disease, diabetes, cancer, and so on.[23] Quercetin is an acidic drug, and thus its solubility increases with pH. Polymer science has great potential to develop novel drug delivery systems, particularly those capable of controlled release.[24,25] Hydrophilic polymers such as PVP, polyvinyl alcohol, polyethylene glycol and poly(ethylene oxide) have been widely explored as carriers of poorly water soluble drugs, with

the aim of developing new types of SDs.[26-28] In this work, PVP, one of the most widely used polymers in pharmaceutics, was selected as filament-forming matrix for nanofiber preparation.[27,28]

2. Experimental

2.1. Materials

Quercetin (purity > 98%, No. MUST-12072505) was purchased from the Beijing Aoke Biological Technology Co. Ltd. (Beijing, China). PVP K60 (M=360,000) was purchased from the Shanghai Yunhong Pharmaceutical Aids and Technology Co., Ltd. (Shanghai, China). Citric acid monohydrate, sodium hydroxide, and anhydrous ethanol were purchased from the Sinopharm Chemical Reagent Co. Ltd. (Shanghai, China). All other chemicals used were analytical grade. Water was double distilled before use.

2.2. Coaxial electrospinning

The shell fluid consisted of 8.0 g of PVP K60 and 1.40 g citric acid monohydrate dissolved in 100 mL of ethanol. Two different core fluids were used in this study: one consisted of 8.0 g of PVP K60, 0.40 g sodium hydroxide, and 2.5 g quercetin in ethanol/water (50/50 v/v; 100 mL total volume), and the other of 8.0 g of PVP K60, 0.40 g sodium hydroxide, and 5.0 g quercetin in ethanol/water (50/50 v/v; 100 mL total volume).

Two syringe pumps (KDS200 and KDS100, Cole-Parmer, Vernon Hills. IL, USA) and a high-voltage power supply (ZGF 60 kV/2 mA, Shanghai Sute Corp., Shanghai, China) were employed in electrospinning. A homemade concentric spinneret was used to conduct both single fluid (adjusting the core or shell fluid flow rate to zero mL/h) and coaxial electrospinning processes. This spinneret was prepared by inserting a small stainless steel tube (27G, outer and inner diameters are 0.42 and 0.21mm respectively) into a larger stainless steel tube (18G, outer and inner diameters of 1.25 and 0.84,mm). The inner tube protrudes 0.2 mm from the outer tube.

Table 1 Details of the electrospinning processes and resultant products

No.	Electrospinning process	Fluid flow rate (mL/h)		Morphology	Size (μm)
		Shell [a]	Core		
F1	Single fluid	--	1.0 [b]	--	--
F2	Single fluid	1.0	--	Nanofibers	0.63±0.11
F3	Coaxial	0.5	0.5 [b]	Nanofibers	0.74±0.18
F4	Coaxial	0.5	0.5 [c]	Nanofibers	0.76±0.22

[a] The shell fluid consisted of 8.0 g of PVP K60 and 1.40 g citric acid monohydrate in 100 mL ethanol.

[b] This core fluid consisted of 8.0 g of PVP K60, 0.40 g sodium hydroxide, and 2.5 g quercetin in 100 mL water/ethanol (50/50 v/v).

[c] Core fluid consisted of 8.0 g of PVP K60, 0.40 g sodium hydroxide, and 5.0 g quercetin in 100 mL water ethanol (50/50 v/v).

Experiments were recorded using a digital video recorder (PowerShot A490, Canon, Tokyo, Japan) under 11× magnification. After initial optimization, the applied voltage was fixed at 12 kV, and the nanofibers collected on aluminum foil at a distance of 15 cm. All other parameters are listed in Table 1. The products were dried for at least 24 h at 40 °C under vacuum (320 Pa) in a DZF-6050 electric vacuum drying oven (Shanghai Laboratory Instrument Work Co. Ltd, Shanghai, China) to facilitate the removal of residual organic solvent and moisture. They were then stored in a desiccator before characterization was undertaken.

2.3. Characterization

2.3.1. Morphology

The morphology of the nanofibers was examined using an S-4800 field-emission scanning electron microscope (FESEM, Hitachi, Tokyo, Japan). Prior to examination, the samples were platinum sputter-coated under a nitrogen atmosphere to render them electrically conductive. The average fiber diameter was determined by measuring their sizes in FESEM images at more than 100 different places, using the ImageJ software (National Institutes of Health, Bethesda, MD, USA).

Transmission electron microscope (TEM) images of the core-shell nanofibers F3 and F4 were recorded on a JEM 2100F field-emission instrument (JEOL, Tokyo, Japan). Samples for TEM were prepared by fixing a lacey carbon-coated copper grid directly onto the collector and electrospinning onto it for several minutes.

The topographies of raw quercetin powder and fibers F3 and F4 were observed under cross-polarized light using an XP-700 polarized optical microscope (Shanghai Changfang Optical Instrument Co. Ltd, Shanghai, China).

2.3.2. Physical status and compatibility

X-ray diffraction (XRD) was performed on a D/Max-BR diffractometer (RigaKu, Japan) with Cu Kα radiation in the 2θ range of 5°–60° at 40 mV and 30 mA. Attenuated total reflectance Fourier transform infrared (ATR-FTIR) analysis was undertaken on a Nexus 670 FTIR spectrometer (Nicolet Instrument Corporation, Madison, WI, USA) over the range of 500 - 4000 cm^{-1} and at a resolution of 2 cm^{-1}.

2.3.3. In vitro dissolution tests

To explore the pH changes induced by dissolution, 10 mL of doubly distilled water was placed in a Petri dish with a diameter of 10 cm. A piece of the nanofiber mats (F2, F3 and F4) with a size of 3 × 3 cm was added to the water. After dissolution, a PHBJ-260 pH meter (Shanghai Jingke Industrial Co. Ltd., Shanghai, China) was exploited to determine the pH value and also a pH test paper was placed into the Petri dish to provide a visual effect. The processes were recorded using a digital video recorder (details as above).

In vitro dissolution tests were carried out according to the Chinese Pharmacopoeia, 2010 ed. Method II, a paddle method, was performed using a RCZ-8A dissolution apparatus (Tianjin University Radio Factory, Tianjin, China). Formulations containing equal amounts of quercetin (i.e. 30 mg raw powder, 244 mg of fiber F3 and 137 mg of F4) were placed in 900 mL of physiological saline (PS, 0.9 wt %) at 37 ± 1 °C. The instrument was set to stir at 50 rpm, providing sink conditions with $C < 0.2C_s$. At predetermined time points, 5.0 mL aliquots were withdrawn from the dissolution medium and replaced with fresh medium to maintain a constant volume. After filtration through a 0.22 μm membrane (Millipore, Billerica, MA, USA) and appropriate dilution with PS, the samples were analyzed at λ_{max} = 371 nm using a UV/vis spectrophotometer (UV-2102PC, Unico

Instrument Co. Ltd., Shanghai, China). The cumulative amount of quercetin released was calculated from the data obtained with a predetermined calibration curve. Experiments were carried out six times, and the cumulative percent released reported as mean values ± S.D.

3. Results and discussion

3.1. Strategy for the preparation of AB-SDs

A diagrammatic sketch depicting the preparation of AB-SDs using coaxial electrospinning is shown in Fig. 1. The strategy comprises three steps: (1) to enhance the solubility of the drug, basic solutions of the drug and polymer were prepared, together with a separate solution containing an equal amount of citric acid and polymer; (2) coaxial electrospinning processes were carried out with the drug-free citric acid / polymer solution as the shell fluids to encapsulate the drug-containing core; and (3) the core-shell nanofiber AB-SDs were dried in an oven to remove solvent residues.

Sharing characteristics of both electrospraying and conventional solution dryspinning, electrospinning can convert the working solutions into solid materials extremely rapidly, often on the time scale of 10^{-2} s. [29, 30] Electrospinning is thus an appropriate method for preparing nanocomposites. [31] Coaxial electrospinning can duplicate the concentric structure of the spinneret into the nanoscale. The components in the shell and core fluids are propagated almost exclusively into the shell and core parts of the fibers. It is also able to 'freeze' the drug molecules into a state comparable to a liquid form. This can be very useful to prevent phase separation or re-crystallization of drug.

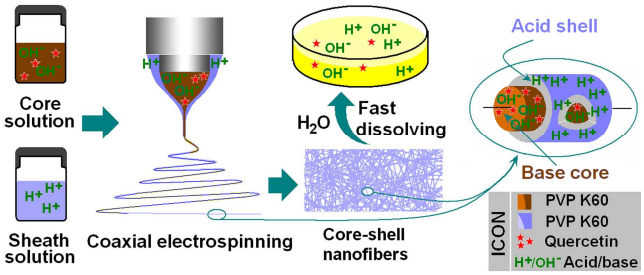

Fig. 1 A schematic showing the preparation of AB-SDs using a coaxial electrospinning process

3.2. The coaxial electrospinning process

Photographs of the single fluid and coaxial electrospinning processes are given in Fig. 2. A digital image of the apparatus is illustrated in Fig. 2a; the insets show the core and shell solutions. The connection between the power supply and the spinneret, and the connection between the spinneret with the core and shell syringe pumps are provided in Fig. 2b and Fig. 2c.

When the flow rate of the shell fluid was adjusted to 0 mL/h, It was a single fluid electrospinning of the core solution. This process is depicted in Fig. 2d: the fluid behaviour is very typical exhibiting a Taylor cone, followed by a straight jet and then a bending and whipping process. Single fluid electrospinning of the shell solution alone and co-axial electrospinning of the shell and core solutions also generated these typical fluid behaviours. However, there are several differences between them, which include: 1) The Taylor cone of the core fluid when spun alone was brown in colour, while that of the shell fluid alone was transparent. The compound Taylor cone in the coaxial process exhibited a yellowish-black colour, and the core solution is seen to be well encapsulated by the shell; 2) The straight fluid jets had different lengths: the core and shell fluids spun alone had lengths of 2.7 mm and 9.4 mm, respectively. Their combination in the coaxial process led to a jet of an intermediate length, 2.8 mm. 3) The fiber mats of F2 and F3 had a white colour, whereas those of F1 had a slight brown colour. This indicates that the quercetin-containing core was well encapsulated by the shell part in the core-shell F3 fibers.

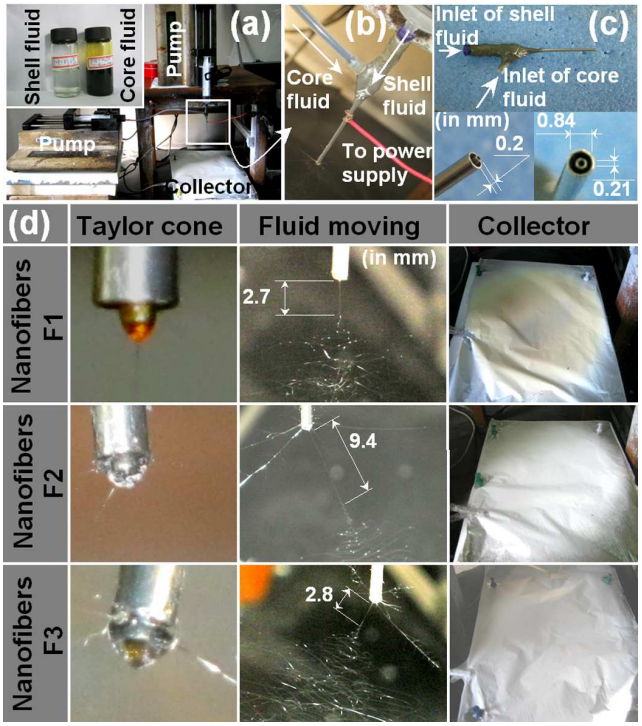

Fig. 2 Coaxial electrospinning of the acid/base solutions: (a) Digital image showing the apparatus arrangement; (insets show the core and shell solutions); (b) the connection between the power supply and the spinneret; (c) the homemade concentric spinneret; (d) visual observations of the Taylor cone, the fluid moving, and the collected fibers.

After drying, the mats of F2, F3 and F4 could be easily peeled from the aluminium foil. However, F1 was strongly bound to the foil and could not be removed easily. This suggested that the solvent in the core fluid (most probably the water) did not fully evaporate during the electrospinning process

3.3. Morphology and structure of the nanofibers

The morphologies of all four nanofiber formulations are shown in Fig. 3. Other than F1, the fibers have smooth surfaces and uniform structures without any beads-on-a-string or spindles-on-a-string morphologies. No drug nanoparticles could be discerned on the surface of F2, F3, or F4. The F2 fibers prepared by spinning the shell fluid alone had average diameters of 630 nm ± 110 nm (Table 1; Fig. 3b). The core-shell nanofibers F3 and F4

had average diameters of 740 nm ± 180 nm (Table 1; Fig. 3c) and 760 nm ± 220 nm (Table 1; Fig. 3d), respectively. Consistent with the observations detailed above in Section 3.2, F1 (from electrospinning of the core fluid alone) could not be totally solidified: residual solvent in the fiber mat led to their binding together on the collector, retaining vestiges of a fiber morphology only on the surface (Fig. 3a).

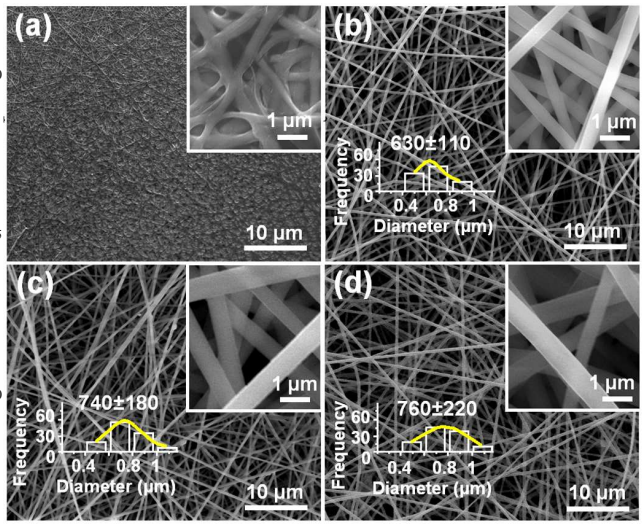

Fig. 3 FESEM images of the electrospun fibers and their diameter distributions. (a) F1, from single fluid electrospinning of the core solution; (b) F2, from single fluid electrospinning of the shell solution; (c) F3; and, (d) F4, both produced by co-axial electrospinning. The insets show an enlarged image of the corresponding nanofibers.

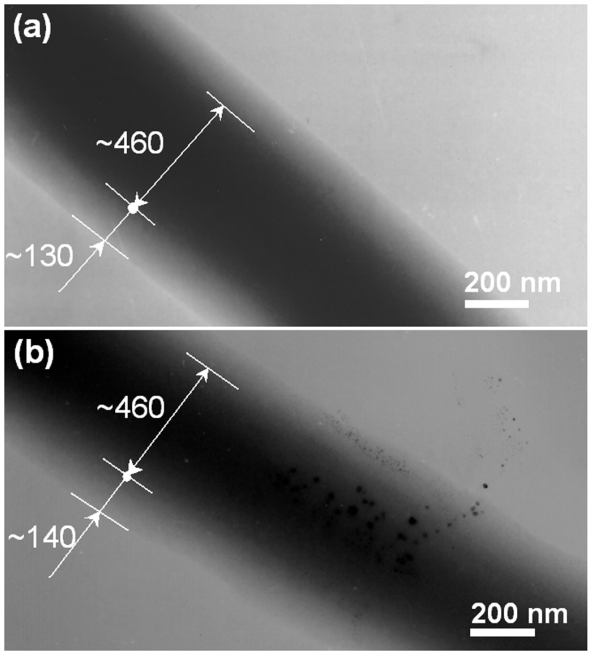

Fig. 4 TEM images of the core-shell nanofibers (a) F3 and (b) F4.

Fig. 4 shows TEM images of the coaxial fibers F3 and F4. Both have clear core-shell structures, with the core and shell segments of each having similar sizes (the cores of both are estimated to be 460 nm and the shells 130 nm and 140 nm for F3 and F4, respectively). No particles could be discerned in the core of F3, suggesting a homogeneous structure (Fig. 4a). However, with the increased drug content of F4, solid phase separation was observed occasionally. As depicted in Fig. 4b. These of nanoparticles presumably formed during the electrospinning process and have penetrated both into the fiber shell and out of the fibers.

3.4. Physical state and compatibility of components

The presence of numerous distinct reflections in its XRD pattern proves that the active ingredient quercetin exists as a crystalline material (see Fig. 5). This is also confirmed by the observation of colourful images when raw quercetin powders are viewed under polarized light. The quercetin crystals are chromatic under cross polarized light, while in sharp contrast the fibers shows no resolvable colour of drug crystals under a magnification of 20×40 (Fig. 5).

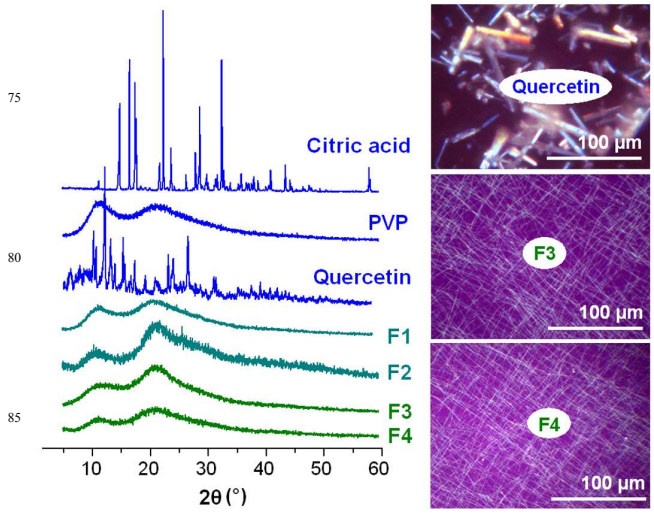

Fig. 5 XRD patterns of the raw materials and fibers, and cross-polarized light observations of quercetin and F3 and F4.

The XRD pattern of citric acid monohydrate also displays many Bragg reflections, demonstrating its existence as a crystalline material. The PVP diffraction pattern shows a diffuse background pattern with two diffraction halos, as expected given that it is an amorphous polymer.

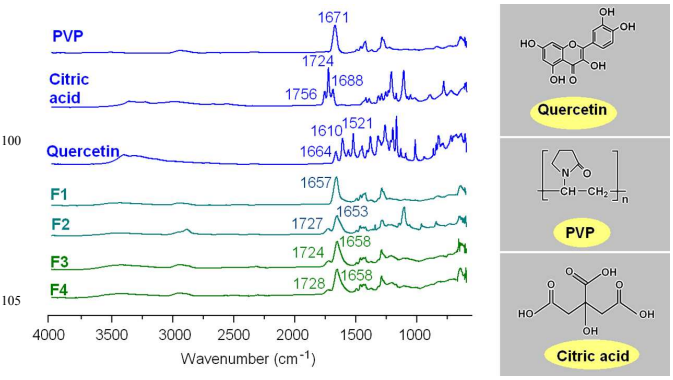

Fig. 6 ATR-FTIR spectra of the raw materials and fibers, and the molecular structures of PVP, quercetin and citrate acid.

The fibers F1 to F4 exhibit none of the characteristic reflections of the starting materials; instead their patterns

comprise the diffuse haloes typical of amorphous materials. The combined XRD and light microscopy results clearly demonstrate that quercetin exists in an amorphous form in the fibers, losing its original crystalline nature. There is no evidence of crystalline material from the nanoparticles observed with F4; this might be because the amount is too small to be detected by XRD, or the nanoparticles may also be amorphous.

Compatibility among the components is very important for producing stable SDs with high quality. Often second-order interactions such as electrostatic interactions, hydrogen bonding, and hydrophobic interactions are desired for improving compatibility. The molecular structures of the main components used in this work are given in Fig. 6. Quercetin and citric acid molecules possess free hydroxyl groups which could act as potential proton donors for hydrogen bonding. PVP can act as proton receptors due to numerous carbonyl groups in its molecules, which result in a characteristic peak at 1671 cm^{-1} in the FTIR spectra (Fig. 6). Therefore it can be postulated that hydrogen bonding should occur within the nanofibers, both in the inner core and in the outer shell.

Quercetin has a characteristic peak of –C=O groups at 1664 cm^{-1} and the three peaks of benzene rings at 1610, 1521 cm^{-1} and a small peak between them. However, all these peaks were absent in the spectra of the nanofibers F1, F3 and F4. Only a single broad peak at 1653, 1658 and 1658 cm^{-1} can be identified for them, respectively, which shows a slight red shift compared to the spectra of pure PVP (Fig. 6). Additionally, almost all peaks in the fingerprint regions of quercetin have shifted, decreased in intensity, or totally disappeared in these nanofibers' spectra. The above-mentioned phenomena suggest that hydrogen bonding occurs between the PVP carbonyl group and the hydroxyl group of the quercetin molecules in nanofibers F1 and the core parts of nanofibers F3 and F4.

Citric acid has three characteristic peaks of –C=O groups at 1756, 1724 and 1688 cm^{-1} resulted from different stretching vibrations of carbonyl groups in the raw crystalline materials (Fig. 6). However, only two characteristic peaks appeared in the spectra of nanofibers F2, F3 and F4. One peak at 1727, 1724 and 1728 cm^{-1} cm^{-1} in the spectra of nanofibers F2, F3 and F4, respectively, is attributed to the stretching vibrations of free carbonyl groups in the loaded citric acid molecules. The other peak at 1653, 1658 and 1658 cm^{-1} suggest that hydrogen bonding occurs between the PVP carbonyl group and the hydroxyl group of the citric acid molecules in nanofibers F2 and the shell parts of nanofibers F3 and F4. And the peak at 1658 cm^{-1} of nanofibers F3 and F4 should be a superposition of their core and shell FTIR responses.

PVP compounds are excellent auxiliaries for the manufacture of effective solid solutions and dispersions by the traditional solvent methods, it has been reported they can enhance the dissolution rates of over 140 poorly water-soluble drugs, and they often exhibit strong ability to inhibit crystallization of dispersed drugs. [32,33] Here, quercetin molecules, by interacting with the polymer PVP, are less likely to form the dimers which are essential for formation of a crystal lattice. This should in turn enhance the stability of these structural nanoproducts for preservations.

3.4. *In vitro* dissolution tests

The fibers of F3 and F4 disappeared instantly after they were placed in the dissolution medium. This effect is attributed to the PVP polymer matrix being highly hygroscopic and hydrophilic, while in addition the nanofibers have very large surface areas, small diameters, and exist as a porous web structure. Finally, the encapsulated quercetin exists in the amorphous form, meaning there is no lattice energy barrier to dissolution. Photographs of the dissolution process of F4 are given in Fig. 7a. The entire process was complete in 18.7 ± 3.4 s (n=3). When the F4 fibers were totally dissolved, the dissolution medium was neutral with a pH value of 6.9 (see Fig. 7b, left side). In contrast, the dissolution solution from F2 was acidic with a pH value of 3.2 (Fig. 7b, right side).

Since quercetin has a UV absorbance peak at λ_{max} = 371 nm, the amount of quercetin released from the fibers is easily determined by UV spectroscopy using a predetermined calibration curve: $C = 15.95A - 0.0017$ ($R^2 = 0.9997$), where C is the quercetin concentration (μg/mL) and A is the solution absorbance at 371 nm (linear range: 2μg/mL to 20μg/mL).

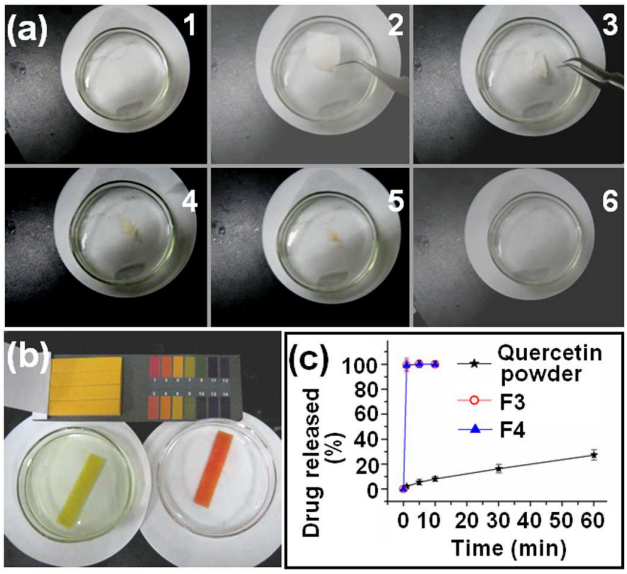

Fig. 7 *In vitro* dissolution tests. (a) Photographs of the dissolution of F4, which is shown in sequence from 1 to 6 and complete within 20 s; (b) The pH value of deinonised water after the dissolution of F2 (right) and F4 (left); (c) *in vitro* release profiles of quercetin (n=6).

The *in vitro* drug release profiles of F3, F4 and the raw quercetin powder (particle size smaller than 100 μm) are provided in Fig. 7c. The core-shell nanofibers F3 and F4 exhibited extremely rapid release of the incorporated quercetin, freeing all the drug within one minute. In comparison, the crude quercetin particles dissolved slowly, only reaching 28.9% release in one hour. Although the nanofibers F3 and F4 had different weights and different diameters, they were able to release all the contained drugs similarly in one minute. This suggests that the amorphous status of quercetin in the core-shell SDs had played a dominant role during the in vitro dissolution processes, let the

drug synchronously dissolve with the polymer matrix through an erosion mechanism. Additionally, the final release amounts of quercetin from the core-shell nanofibers F3 and F4 were 30.2 ± 1.3 mg and 30.1 ± 1.1 mg, respectively, almost equivalent to the calculated value, indicating no drug loss during the coaxial electrospinning processes.

Accelerated dissolution of drugs, particularly those with poor water solubility, is highly sought after to enhance their pharmaceutical applications.[20,21,34] The high surface area, narrow diameters and high porosity of electrospun fiber mats have been explored for different types of applications where rapid onset of action is required.[10,35] This work opens a route for developing fast dissolving drug delivery systems. The AB-SDs of quercetin produced here could be further processed into fast disintegrating membranes for sublingual drug delivery or capsules for oral administration. Certainly, because quercetin is fragile in a basic condition,[36] its chemical and physiological stability, and the physical stability of AB-SDs should be systematically investigated before the development of commercial products.

4. Conclusion

The dissolution of poorly water-soluble drugs is one of the most challenging aspects in the development of new medicines. In this work, a new type of acid-base pair solid dispersions (AB-SDs) was developed to enhance the dissolution rate of an acidic drug. Poly(vinylpyrrolidone) was used as the polymer matrix and quercetin as a model drug, AB-SDs of quercetin in the form of core-shell nanofibers were fabricated using coaxial electrospinning. Scanning electron microscopy images showed that the nanofibers were linear without any beads-on-a-string morphology. Transmission electron microscopy images revealed the fibers to have clear core-shell structures. X-ray diffraction demonstrated that the active ingredient was present in the fibers in an amorphous state, which might be attributed to the rapid evaporation of solvent in the electrospinning process and also the favourite secondary interactions between the drug and the polymer matrix suggested by infrared spectroscopy. In *in vitro* dissolution tests, the drug was released immediately when the core-shell nanofibers encountered the dissolution medium. When the AB-SD fibers were added to deionised water, the medium remained remained after dissolution due to the presence of an acid-base pair in the fibers. This study therefore demonstrates the systematic design, preparation, characterization and application of a new type of SD to improving the dissolution properties of poorly water soluble drugs.

Acknowledgments

This work was supported by the National Science Foundation of China (No. 51373101), the China NSFC/UK Royal Society cost share international exchanges scheme (No. 51411130128), the Natural Science Foundation of Shanghai (No. 13ZR1428900) and the Key Project of the Shanghai Municipal Education Commission (No.13ZZ113).

Notes and references

[a] *Research Center for Analysis and Measurement, Donghua University, Shanghai 201620, China. Tel: 86(21) 67792047; E-mail: yanjie01@eyoul.com (J Yan),*

[b] *The Department of Mechanical Engineering, Guangxi Technological College of Machinery and Electricity, Nanning 530007, China.*

[c] *School of Materials Science & Engineering, University of Shanghai for Science and Technology, Shanghai 200093, China. Fax: 86(21) 55270632; Tel: 86(21) 55274069; E-mail: ydg017@usst.edu.cn (DG Yu),*

[d] *UCL School of Pharmacy, 29-39 Brunswick Square, London, WC1N 1AX, UK; E-mail: g.williams@ucl.ac.uk (GR Williams)*

1. G. S. Anjusree, A. Bhupathi, A. Balakrishnan, S. Vadukumpully, K. R. V. Subramanian, N. Sivakumar, S. Ramakrishna, S. V. Nair and A. S. Nair. *RSC Adv.*, 2013, **3**, 16720-16727.
2. E. Atabey, S. Wei, X. Zhang, H. Gu, X. Yan, Y. Huang, L. Shao, Q. He, J. Zhu, L. Sun, A. S. Kucknoor, A. Wang and Z. Guo. *J. Compos. Mater.*, 2013, **47**, 3175-3185.
3. S.L. Liu, Y.Z. Long, Y.Y. Huang, H.D. Zhang, H.W. He, B. Sun, Y.Q. Sui and L.H. Xia. *Polym. Chem.*, 2013, **4**, 5696-5700.
4. J. Sharma, X. Zhang, T. Sarker, X. Yan, L. Washburn, H. Qu, Z. Guo, A. Kuckoor and S. Wei. *Polymer*, 2014, **55**, 3261-3269.
5. J. Zhu, M. Chen, Q. He, L. Shao, S. Wei and Z. Guo. *RSC Adv.*, 2013, **3**, 22790-22824.
6. F. Zheng, S. Wang, M. Shen, M. Zhu and X. Shi. *Polym. Chem.*, 2013, **4**, 933-941.
7. C. Su, Y. Tong, M. Zhang, Y. Zhang and C. Shao. *RSC Adv.*, 2013, **3**, 7503-7512.
8. C. L. Zhang and S. H. Yu. *Chem. Soc. Rev*., 2014, DOI: 10.1039/C3CS60426H.
9. H. Yang, P.F. Gao, W.B. Wu, X.X. Yang, Q.L. Zeng, C. Li and C.Z. Huang. *Polym. Chem*., 2014, **5**, 1965-1975.
10. D. G. Yu, F. Liu, L. Cui, Z. P. Liu, X. Wang and S. W. A. Bligh. *RSC Adv.*, 2013, **3**, 17775-17783.
11. A. K. Moghe and B. S. Gupta. *Polym. Rev*., 2008, **48**, 353-377.
12. P. Zhang, C. Shao, X. Li, M. Zhang, X. Zhang, C. Su, N. Lu, K. Wang and Y. Liu. *Phys. Chem. Chem. Phys.*, 2013,**15**, 10453-10458.
13. S. Agarwal, A. Greiner and J. H. Wendorff. *Prog. Polym, Sci.* 2013, **38**, 963–991.
14. C. Li, Z. H. Wang, D. G. Yu and G. R. Williams. *Nanoscale Res. Lett*., 2014, **9**, 258.
15. D. G. Yu, J. H. Yu, L. Chen, G. R. Williams and X. Wang.. *Carbohydr. Polym.*, 2012, **90**, 1016-1023.
16. H. Chen, N. Wang, J. Di, Y. Zhao, Y. Song and L. Jiang. *Langmuir*, 2010, **26**, 11291-11296.
17. Z. K. Nagy, A. Balogh, G. Drávavölgyi, J. Ferguson, H. Pataki, B. Vajna and G. Marosi. *J. Pharm. Sci*., 2013, **102**, 508-517.
18. W. Lu, J. Sun and X. Jiang. *J. Mater. Chem. B*, 2014, **2**, 2369-2380.
19. D. G. Yu, X. X. Shen, C. Brandford-White, K. White, L. M. Zhu and S. W. A. Bligh. *Nanotechnology*, 2009, **20**, 055104.
20. D. G. Yu, J. M. Yang, C. Branford-White, P. Lu, L. Zhang and L. M. Zhu. *Int. J. Pharm.*, 2010, **400**, 158-164.
21. D. G. Yu, L. M. Zhu, C. Branford-White, J. H. Yang, X. Wang, Y. Li and W. Qian. *Int. J. Nanomed.*, 2011, **6**, 3271-3280.
22. H. Chen, J. Wan, Y. Wang, D. Mou, H. Liu, H. Xu and X. Yang. *Nanotechnology*, 2008, **19**, 375104.
23. H. L. Li, X. B. Zhao, Y. K. Ma, G. X. Zhai, L. B. Li and H. X. Lou. *J. Control. Release*, 2009, **133**, 238–244.
24. S. Demirci, A. Celebioglu, Z. Aytac and T. Uyar. *Polym. Chem*., 2014, **5**, 2050-2056.
25. L. Cui, Z.P. Liu, D.G. Yu, S.P. Zhang, S.W.A. Bligh and N. Zhao. *Colloid. Polym. Sci.*, 2014, DOI:10.1007/s00396-014-3226-8.
26. X. Hu , S. Liu, G. Zhou, Y. Huang, Z. Xie and X. Jing. *J. Control.*

Release, 2014, **185**, 12-21.
27. T. Vigh, T. Horváthová, A. Balogh, P. L. Sóti, G. Drávavögyi, Z. K. Nagy and G. Marosi. *Eur. J. Pharm. Sci.*, 2013, **49**, 595-602.
28. M. Chen, H. Qu, J. Zhu, Z. Luo, A. Khasanov, A. S. Kucknoor, N. Haldolaarachchige, D. P. Young, S. Wei and Z. Guo. *Polymer*, 2012, 53, 4501-4511.
29. O. V. Salata. *Curr. Nanosci.*, 2005, **1**, 25-33.
30. D. Li and Y. Xia. *Adv. Mater*., 2004, **16**, 1151-1170.
31. X. Lu, W. Zhang, C. Wang, T. C. Wen and Y. Wei. *Prog. Polym. Sci*., 2011, **36**, 671-712.
32. V. Bühler. Kollidon: Polyvinylpyrollidone for the Pharmaceutical Industry. 2nd ed. Ludwigshafen: BASF Aktiengesellschaft Feinchemie, 1998.
33. C. Leuner and J. Dressman. *Eur. J. Pharm. Biopharm*., 2000, **50**, 47–60.
34. J. L. Manasco, C. Tang, N. A. *RSC adv*., 2014, **4**, 13274-13279
35. G. Fu, Z. Su, X. Jiang and J. Yin. *Polym. Chem*., 2014,**5**, 2027-2034.
36. Y. J. Moon, L. Wang, R. DiCenzo and M. E. Morris. *Biopharm. Drug Dispos*., 2008, **29**, 205-217.